Supporting Information

Isomerization Strategy on Non-fullerene Guest Acceptor Enables Stable Organic Solar Cells over 19% Efficiency

Zhenyu Chen,[a,b] Jintao Zhu,[c] Daobin Yang,[a,b,*] Wei Song[a,b*], Jingyu Shi,[a,b] Jinfeng Ge,[a,b] Yuntong Guo,[a] Xinyu Tong,[a,b] Fei Chen,[c] Ziyi Ge[a,b,*]

[a] Zhejiang Engineering Research Center for Energy Optoelectronic Materials and Devices, Ningbo Institute of Materials Technology and Engineering, Chinese Academy of Sciences, Ningbo 315201, China.

[b] Center of Materials Science and Optoelectronics Engineering, University of Chinese Academy of Sciences, Beijing 100049, China.

[c] Department of Chemical and Environmental Engineering, University of Nottingham Ningbo China, Ningbo 315100, China

E-mail: *yangdaobin@nimte.ac.cn; songwei@nimte.ac.cn; geziyi@nimte.ac.cn*

1. Experimental section

1.1 Instruments and characterization

^{1}H NMR spectra were recorded on Bruker (AVANCE III 400MHz). High resolution time of flight mass spectrometer (HR-TOF-MS) was obtained from AB Sciex (TripleTOF 4600). Thermogravimetric analysis (TGA) was under taken using a PerkinElmer (Diamond TG/DTA) under N_2 atmosphere at a heating rate of 10 °C min^{-1}. Differential scanning calorimetry (DSC) measurement was performed on TG-DSC (STA 449F3) under Ar atmosphere at a heating rate of 10 °C min^{-1}. Absorption spectra of the thin-film samples of these materials were recorded using a Perkin Elmer (Lamdba 950) UV-Vis scanning spectrophotometer. The film samples were obtained by spin-coating from chloroform solution on quartz substrates.

The morphologies of the active layers were analyzed through atomic force microscopy (AFM) in tapping mode under ambient conditions using Bruker (Dimension ICON) instrument. Photoinduced force microscope (Pi-FM) measurements were performed on NanoIR2-fs at Shandong University. GI-WAXS measurements were performed on a XEUSS SAXS/WAXS system (XENOCS, France) at the National Center for Nanoscience and Technology. The wavelength of the X-ray beam is 1.54 Å, and the incident angle was 0.18°. Scattered X-rays were detected by using a Dectris Pilatus 300 K photon counting detector. The blend films for GI-WAXS and AFM were made by the same method for device active layer except for the substrate as Si/PEDOT:PSS.

1.2 Cyclic voltammetry (CV)

The energy levels for N3, QX-α and QX-γ were measured by cyclic voltammetry (CV) using a PC controlled 604E electrochemical workstation, which was performed by using Ag/AgCl as reference electrode in 0.1 mol L^{-1} tetra-*n*-butylammonium hexafluorophosphate (*n*-Bu_4NPF_6) solution, and ferrocene/ferrocenium (Fc/Fc^+) (-0.1 eV versus Ag/AgCl) was used as internal reference. The CV system was constructed using a Pt disk as the working electrode, a Pt wire as the counter electrode, and a

$Ag/AgNO_3$ (0.1 mol L^{-1} in acetonitrile) electrode as the reference electrode. The HOMO and LUMO were calculated according to the following equations:

$$\text{HOMO} = -[E_{ox}^{onest} + 4.8\ ]$$

$$\text{LUMO} = -[E_{red}^{onest} + 4.8\ ]$$

Where E_{ox}^{onset} and E_{red}^{onest} are the onset of oxidation potential and reduction potential *vs.* Fe/Fe^{+}, respectively.

1.3 Device fabrication and characterizations

1.3.1 Rigid OSCs fabrications

The OSC was fabricated with the traditional sandwich structure: ITO/ PEDOT: PSS /active layer /PDINN /Ag. Firstly, the chloroform solution containing D18 and acceptors with a ratio of 1:1.3 was stirred at 60 ℃ for 5 hours in the nitrogen-filled glovebox. After being cleaned with deionized water, acetone and isopropanol, the ITO glass was treated with the UV-Ozone for 20 minutes. The PEDOT: PSS solution was spin-coated at 3000 rpm onto the ITO substrates for 40 seconds. Then the PEDOT:PSS film was heated at 130℃ in air. Then the donor and acceptor were spin-coated with a speed of 3000 r/min on the PEDOT:PSS layer and treated with 150 μL CS_2 in a culture dish with a diameter of 7 cm for 2 min. With the PDINN (1 mg mL^{-1}, 3000r/min) spin-coated on the active layer, the devices were finally transferred to the evaporation tank to deposit 150 nm Ag.

1.3.2 Flexible OSCs fabrication

The structure of the OSCs device was PET/Ag grids/D-PH1000/ PEDOT:PSS/active layer/PDINN/Ag. The PET/Ag NWs first was adhered onto polydimethylsiloxane (PDMS)-coated glass substrates. PH1000 (Clevios, full name: poly(3,4-ethylenedioxythiophene): poly(styrenesulfonate)) with a solid content of 1.0-1.3% show high conductivity and optical transparency as a replacement for transparent conductors such as ITO. PH1000 doped with 1 wt.% D-Sorbitol and 0.5 vol.% PEG-TmDD is referred to as D-PH1000 in this work. PEDOT:PSS (4083) aqueous solution

was then spin-coated at 2500 rpm for 30 s and annealed on a hot stage in the air at 115 ℃ for 20 min. A chloroform solution containing D18:N3: QX-x was prepared to spin coating for fabricating active layer. And the active layer treated with 150 μL CS_2 in a culture dish with a diameter of 7 cm for 2 min. Subsequently, PDINN was dissolved in ethanol solution (1 mg mL^{-1}) and spin-coated at 2000 rpm for 30 s. Finally, Ag was thermally deposited as an electrode at vacuum pressure of ~3×10^{-5} mbar.

1.3.3 Device characterizations

J-V measurements of devices were carried out in the Keithley 2440 source meter with a solar simulator (Newport-Oriel® Sol3A 450W) device. EQE measurements were conducted with the solar cell QE tester (QE-R, Enli Technology Co., Ltd). The active area of OSCs is 4.00 mm^2.

1.3.4 Space charge limited current (SCLC) measurement

Electron-only devices were fabricated using the structure of ITO /Al /active layers / PDINN /Ag. Firstly, after being cleaned with deionized water, acetone and isopropanol, the all-ITO glass was deposited with 100 nm Al and then the D18 and acceptors were spin-coated on the PEDOT:PSS layer and treated with 150 μL CS_2 in a culture dish with a diameter of 7 cm for 2 min. With the PDINN spin-coated on the active layer, the devices were finally transferred to the evaporation tank to deposit 150 nm Ag.

Hole-only devices were fabricated with the structure of ITO /PEDOT: PSS/ active layers /MoO_3 /Ag. After being cleaned with deionized water, acetone and isopropanol, the all-ITO glass was treated with the UV-Ozone for 20 minutes. The PEDOT: PSS solution was spin-coated at 3000 rpm onto the ITO substrates for 40 seconds. Then the PEDOT:PSS film was heated at 130 ℃ in air. Then the donor and acceptor were spin-coated on the PEDOT:PSS layer and treated with 150 μL CS_2 in a culture dish with a diameter of 7 cm for 2 min. Then devices were finally transferred to the evaporation tank to deposit 10 nm MoO_3 and then 150 nm Ag.

1.3.5 Device structure used in storage stability test fabrication

The OSC was fabricated with the structure: ITO/ ZnO /active layer /MoO_3 /Ag. Firstly, the chloroform solution containing D18 and acceptors with a ratio of 1:1.3 was stirred at 60 ℃ for 5 hours in the nitrogen-filled glovebox. After being cleaned with deionized water, acetone and isopropanol, the ITO glass was treated with the UV-Ozone for 20 minutes. The ZnO solution was spin-coated at 4000 rpm onto the ITO substrates for 40 seconds. Then the ZnO film was heated at 150℃ in air. Then the donor and acceptor were spin-coated with a speed of 3000 r/min on the ZnO layer and treated with 150 μL CS_2 in a culture dish with a diameter of 7 cm for 2 min. With 8 nm MoO_3 spin-coated on the active layer, the devices were finally transferred to the evaporation tank to deposit 150 nm Ag.

2. Materials and synthesis

Super dry reagents were purchased from J&K and other conventional reagents were from SCRC. D18 and N3 were purchased from Solarmer Energy Inc. Benzo[1,2-b:4,3-b']dithiophene-4,5-dione and benzo[2,1-b:3,4-b']dithiophene-4,5-dione were from Bide Pharmatech Ltd. INCN-2F was purchased from Nanjing Zhiyan Technology Co., Ltd. 12,13-bis(2-phenylhexyl)-3,9-diundecyl-12,13-dihydro-[1,2,5]thiadiazolo[3,4e]thieno [2",3":4',5']thieno[2',3':4,5]pyrrolo[3,2-g]thieno[2',3':4,5]thieno[3,2-b]indole were purchased from JiangSu GR-Chem Biotech Co., Ltd. The ITO glass was purchased from Suzhou Shangyang Solar Technology Co., Ltd. All reagents were directly used without any further treatment, and all the reactions were carried out under a nitrogen atmosphere.

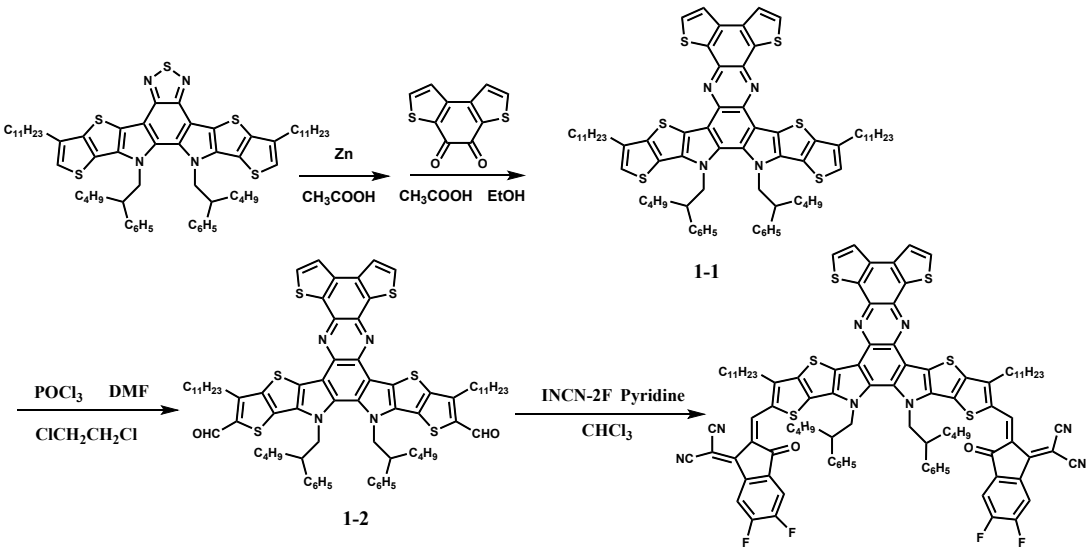

Scheme S1. Synthesis routes of compound QX-α.

Synthesis of compound 1-1: Zinc power (2398.9 mg, 36.91 mmol) was added into a solution of compound 1 (2000 mg, 1.85 mmol) in acetic acid (55 mL) in three-necked flask under nitrogen. Then the mixture was heated to 110 ℃ for 30 min. After the mixture was cooled to room temperature, the solid was removed by filtration. The mixture solution was extracted with dichloromethane. Then the organic phase was removed under reduced pressure and a dark green solid was obtained. The solid was divided into two parks, and half of it and benzo[1,2-b:4,3-b']dithiophene-4,5-dione were added into a mixed solution of EtOH: CH_3COOH=1:1 without further purification. Then the mixture was heated to 110 ℃ for 1 h. After the mixture solution was cooled to room temperature, it was extracted with dichloromethane. The solvent was removed under reduced pressure. Then the organic phase was purified by silica gel column chromatography (PE:DCM=20:1, v/v) to obtain an orange solid 1-1 (420.0 mg, 37%).^{1}H NMR (400 MHz, Chloroform-*d*, ppm) δ: 7.86 – 7.80 (m, 4H), 7.04 (s, 2H), 4.72 (d, *J* = 7.8 Hz, 4H), 2.93 (t, *J* = 7.6 Hz, 4H), 2.20 (q, *J* = 6.5 Hz, 2H), 1.94 (q, *J* = 7.5 Hz, 4H), 1.56 – 1.50 (m, 4H), 1.48 – 1.41 (m, 4H), 1.39 – 1.24 (m, 26H), 1.16 – 0.85 (m, 36H), 0.69 – 0.62 (m, 12H).

Synthesis of compound 1-2: Compound 1-1 (420.0 mg, 0.34 mmol), 1,2-dichloroethane (35 mL), DMF (0.4 mL) were mixed in three-necked flask under nitrogen. $POCl_3$ (0.4 mL) was added dropwise slowly. After reacting at 80 ℃ overnight, the mixture was transferred to a funnel. Then added into saturated Na_2CO_3 solution slowly, and kept stirring. After no bubble, the mixture was extracted with dichloromethane. The organic phase was purified by silica gel column chromatography (PE:DCM=1:2, v/v) to obtain a yellow solid 1-2 (355.0 mg, 81%). ^{1}H NMR (400 MHz, Chloroform-*d*, ppm) δ: 10.17 (s, 2H), 7.85 (d, *J* = 2.3 Hz, 4H), 4.72 (d, *J* = 8.0 Hz, 4H), 3.28 (t, *J* = 7.6 Hz, 4H), 2.17 (dt, *J* = 13.0, 6.9 Hz, 2H), 1.99 (p, *J* = 7.6 Hz, 4H), 1.57 – 1.48 (m, 4H), 1.42 (t, *J* = 7.4 Hz, 4H), 1.38 – 1.19 (m, 26H), 1.14 – 0.83 (m, 36H), 0.69 – 0.60 (m, 12H).

Synthesis of QX-α: compound 1-2 (190.0 mg, 0.15 mmol) and 2-(5,6-difluoro-3-oxo-2,3-dihydro-1H-inden-1-ylidene)malononitrile (116.6 mg, 0.51 mmol) were dissolved in $CHCl_3$. Then pyridine (0.3 mL) was added dropwise slowly under nitrogen, the mixture gradually turned blue and black. After reacting overnight at 60 ℃, the mixture was purified by silica gel column chromatography (PE:CF=1:3, v/v) to obtain a dark blue solid QX-α (153 mg, 60%). ^{1}H NMR (400 MHz, Chloroform-*d*, ppm) δ: 8.97 (s, 2H), 8.23 (s, 2H), 7.82 (t, *J* = 3.6 Hz, 4H), 7.50 (s, 2H), 4.91 (d, *J* = 8.0 Hz, 4H), 3.22 (s, 4H), 2.40 (s, 2H), 1.95 – 1.82 (m, 4H), 1.50 (d, *J* = 13.5 Hz, 8H), 1.43 – 1.13 (m, 46H), 1.13 – 1.00 (m, 13H), 0.85 – 0.79 (m, 6H), 0.76 – 0.68 (m, 10H). HR-TOF-MS (APCI) *m/z*: $[M+H]^+$ calcd. for $C_{100}H_{106}F_4N_8O_2S_6$, 1719.6699; found, 1719.6703.

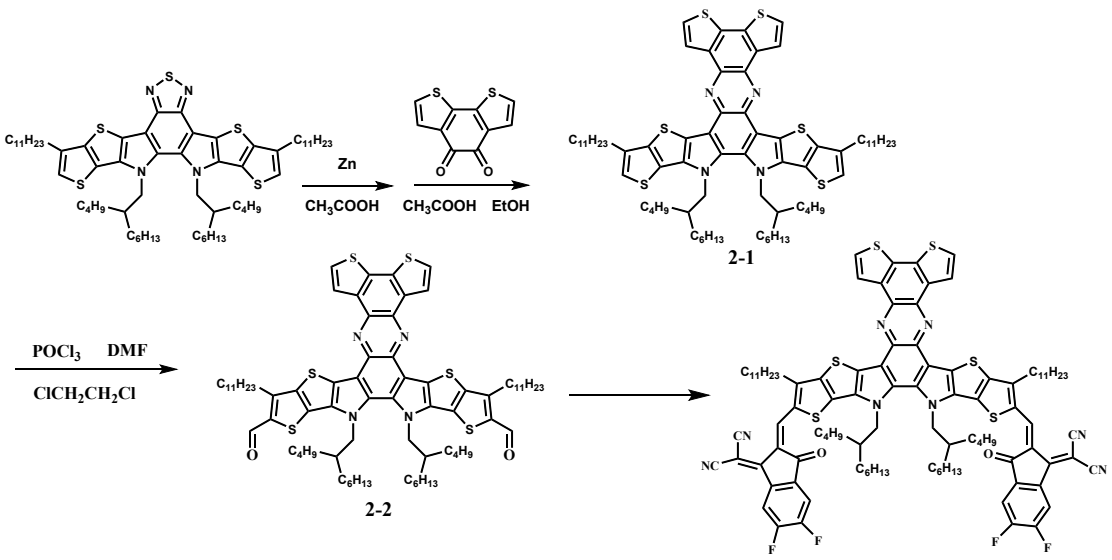

Scheme S2. Synthesis route of compound QX-γ.

Synthesis of compound 2-1: Zinc power (2398.9 mg, 36.91 mmol) was added into a solution of compound 1 (2000 mg, 1.85 mmol) in acetic acid (55 mL) in three-necked flask under nitrogen. Then the mixture was heated to 110℃ for 30 min. After the mixture was cooled to room temperature, the solid was removed by filtration. The mixture solution was extracted with dichloromethane. Then the organic phase was removed under reduced pressure and a dark green solid was obtained. The solid was divided into two parks, and the other half and benzo[2,1-b:3,4-b']dithiophene-4,5-dione were added into a mixed solution of EtOH: CH3COOH=1:1 without further purification. Then the mixture was heated to 110 ℃ for 1 h. After the mixture solution was cooled to room temperature, it was extracted with dichloromethane. The solvent was removed under reduced pressure. Then the organic phase was purified by silica gel column chromatography (PE:DCM=20:1, v/v) to obtain an orange solid 2-1 (360.0 mg, 32%). ^{1}H NMR (400 MHz, Chloroform-*d*, ppm) δ: 8.76 (d, *J* = 5.3 Hz, 2H), 7.66 (d, *J* = 5.3 Hz, 2H), 7.04 (s, 2H), 4.71 (d, *J* = 7.8 Hz, 4H), 2.92 (t, *J* = 7.6 Hz, 4H), 2.20 (q, *J* = 6.5 Hz, 2H), 1.95 (q, *J* = 7.5 Hz, 4H), 1.54 – 1.48 (m, 4H), 1.46 – 1.40 (m, 4H), 1.37 – 1.25 (m, 26H), 1.14 – 0.86 (m, 36H), 0.67 – 0.60 (m, 12H).

Synthesis of compound 2-2: Compound 2-1 (360.0 mg, 0.29 mmol), 1,2-Dichloroethane (30 mL), DMF (0.3 mL) were mixed in three-necked flask under nitrogen. $POCl_3$ (0.3 mL) was added dropwise slowly. After reacting at 80 ℃ overnight, the mixture was transferred to a funnel. Then added into saturated Na_2CO_3 solution slowly, and kept stirring. After no bubble, the mixture was extracted with dichloromethane. The organic phase was purified by silica gel column chromatography (PE:DCM=1:2, v/v) to obtain a yellow solid 2-2 (308.2 mg, 82%). ^{1}H NMR (400 MHz, Chloroform-*d*, ppm) δ: 10.17 (s, 2H), 8.61 (dd, *J* = 5.2, 2.8 Hz, 2H), 7.61 (dd, *J* = 5.2, 2.3 Hz, 2H), 4.75 (d, *J* = 7.9 Hz, 4H), 3.28 (t, *J* = 7.6 Hz, 4H), 2.19 (p, *J* = 6.7 Hz, 2H), 1.99 (p, *J* = 7.6 Hz, 4H), 1.58 – 1.47 (m, 4H), 1.42 (p, *J* = 6.7 Hz, 4H), 1.37 – 1.20 (m, 26H), 1.15 – 0.83 (m, 36H), 0.68 – 0.61 (m, 12H).

Synthesis of QX-γ: compound 2-2 (170.0 mg, 0.14 mmol) and 2-(5,6-difluoro-3-oxo-2,3-dihydro-1H-inden-1-ylidene)malononitrile (116.6 mg, 0.51 mmol) were dissolved in $CHCl_3$. Then pyridine (0.3 mL) was added dropwise slowly under nitrogen, the mixture gradually turned blue and black. After reacting overnight at 60 ℃, the mixture was purified by silica gel column chromatography (PE:CF=1:3, v/v) to obtain a dark blue solid QX-γ (151 mg, 63%). ^{1}H NMR (400 MHz, Chloroform-*d*, ppm) δ: 8.96 (s, 2H), 8.43 (d, *J* = 5.0 Hz, 2H), 8.29 (t, *J* = 8.2 Hz, 2H), 7.61 (d, *J* = 5.1 Hz, 2H), 7.57 (d, *J* = 7.4 Hz, 2H), 4.92 (d, *J* = 8.0 Hz, 4H), 3.16 (s, 4H), 2.38 (s, 2H), 1.85 (t, *J* = 7.7 Hz, 4H), 1.49 (s, 4H), 1.41 – 1.14 (m, 46H), 1.12 – 1.02 (m, 12H), 0.83 – 0.78 (m, 6H), 0.76 – 0.67 (m, 10H). HR-TOF-MS (APCI) *m/z*: $[M+H]^+$ calcd. for $C_{100}H_{106}F_4N_8O_2S_6$, 1719.6699; found, 1719.6724.

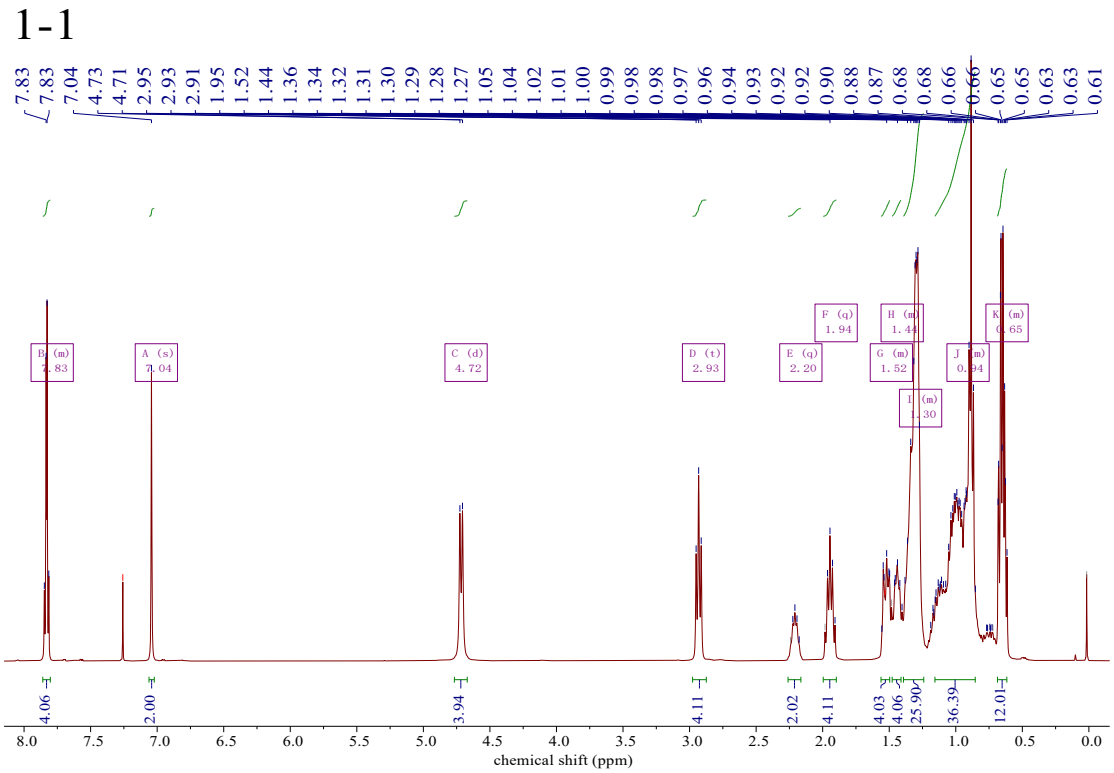

Figure S1. ^{1}H NMR spectrum of compound 1-1 in $CDCl_3$.

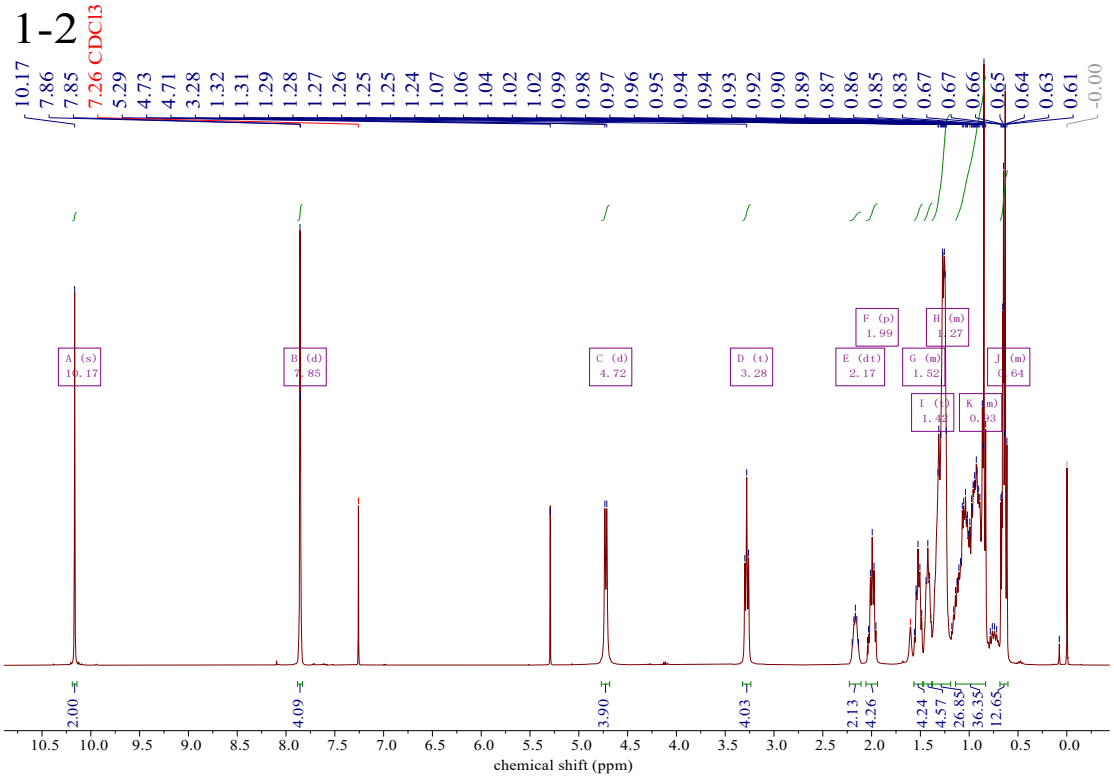

Figure S2. ^{1}H NMR spectrum of compound 1-2 in $CDCl_3$.

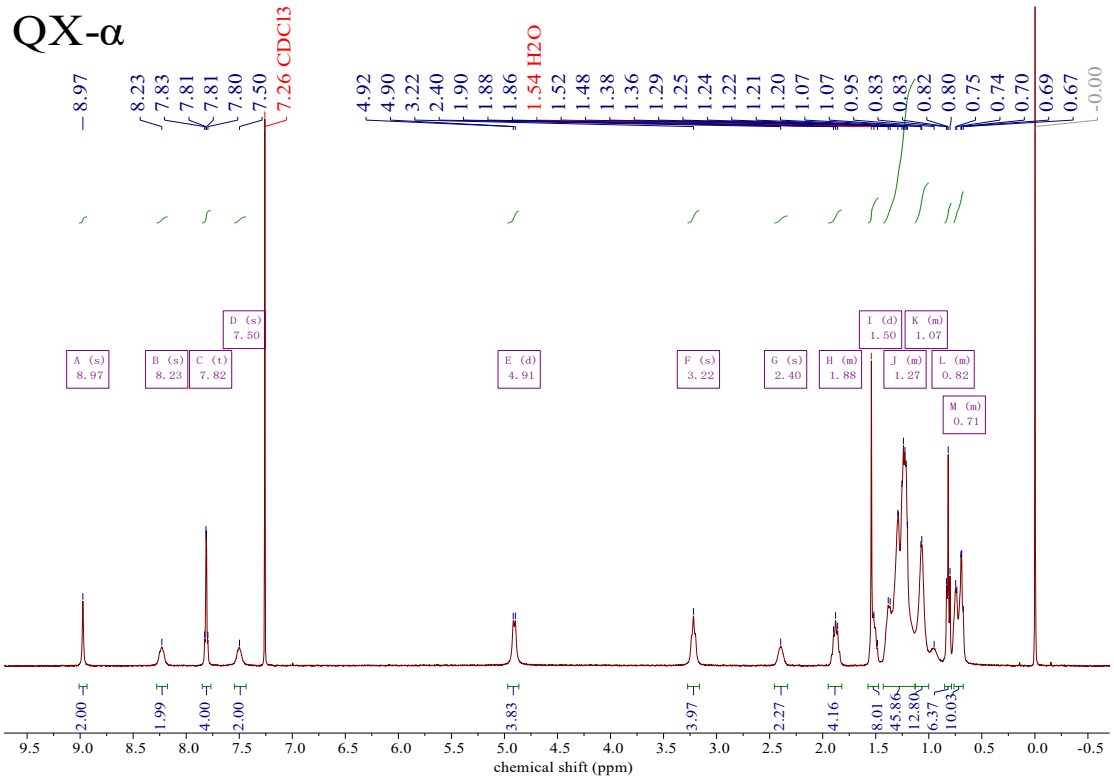

Figure S3. ^{1}H NMR spectrum of QX-α in $CDCl_3$.

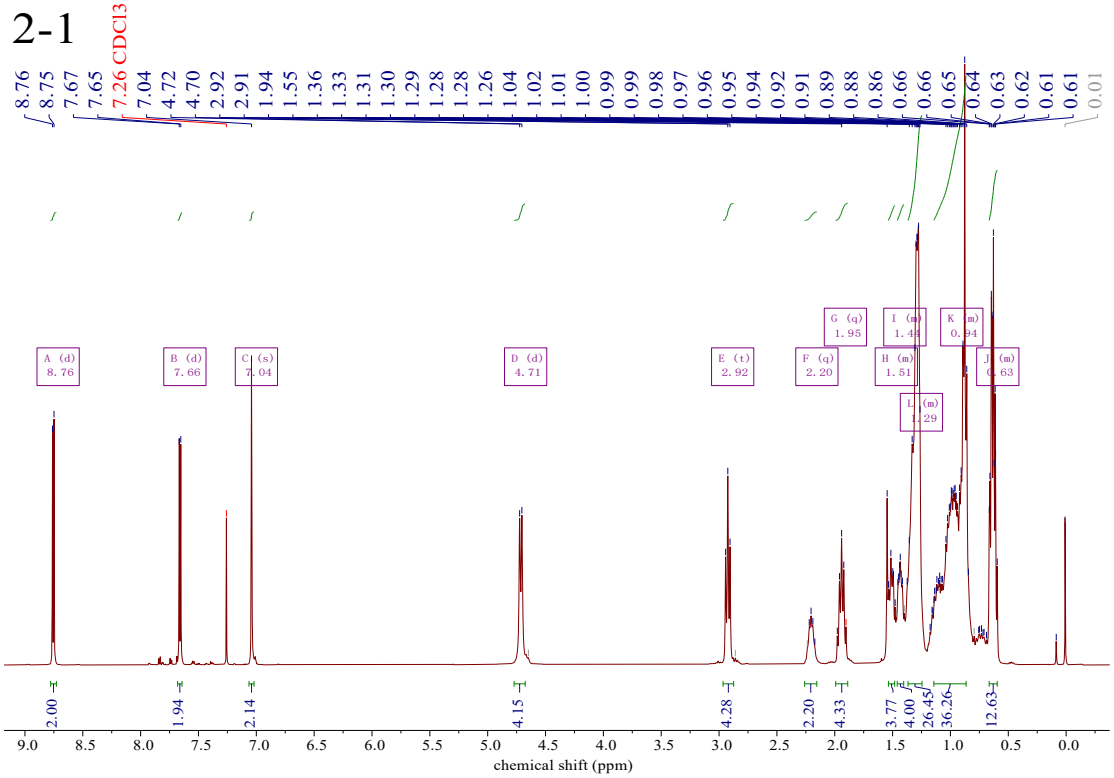

Figure S4. ^{1}H NMR spectrum of compound 2-1 in $CDCl_3$.

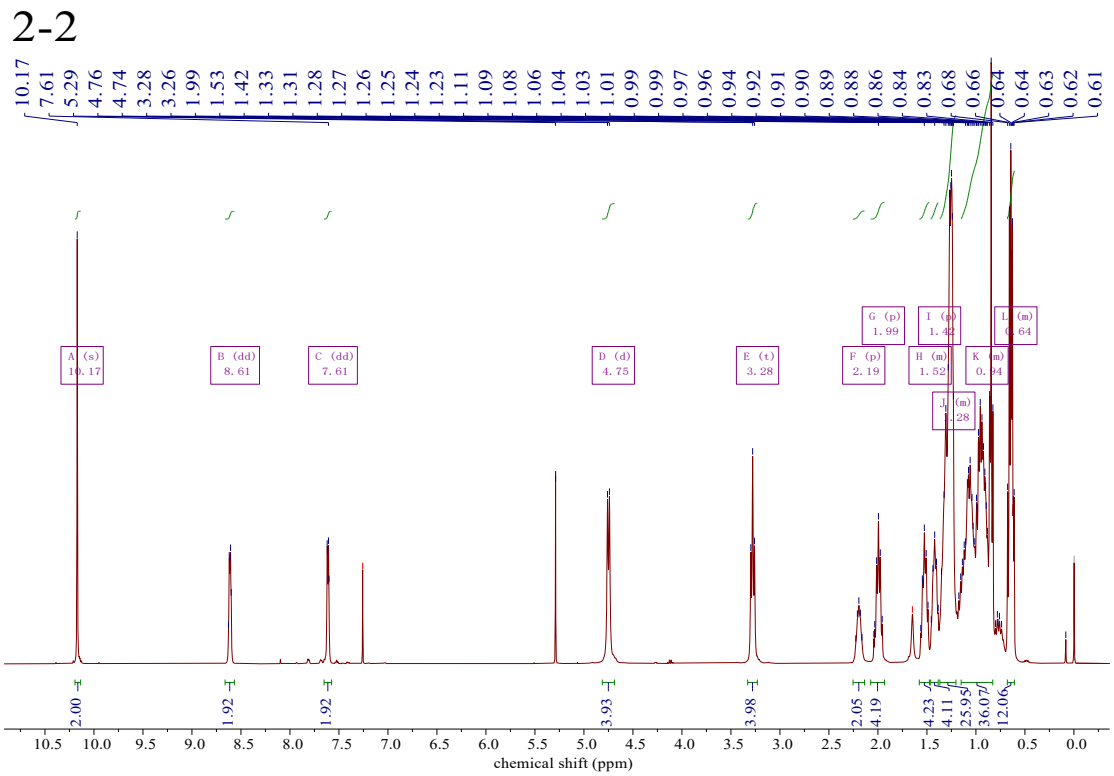

Figure S5. ^{1}H NMR spectrum of compound 2-2 in $CDCl_3$.

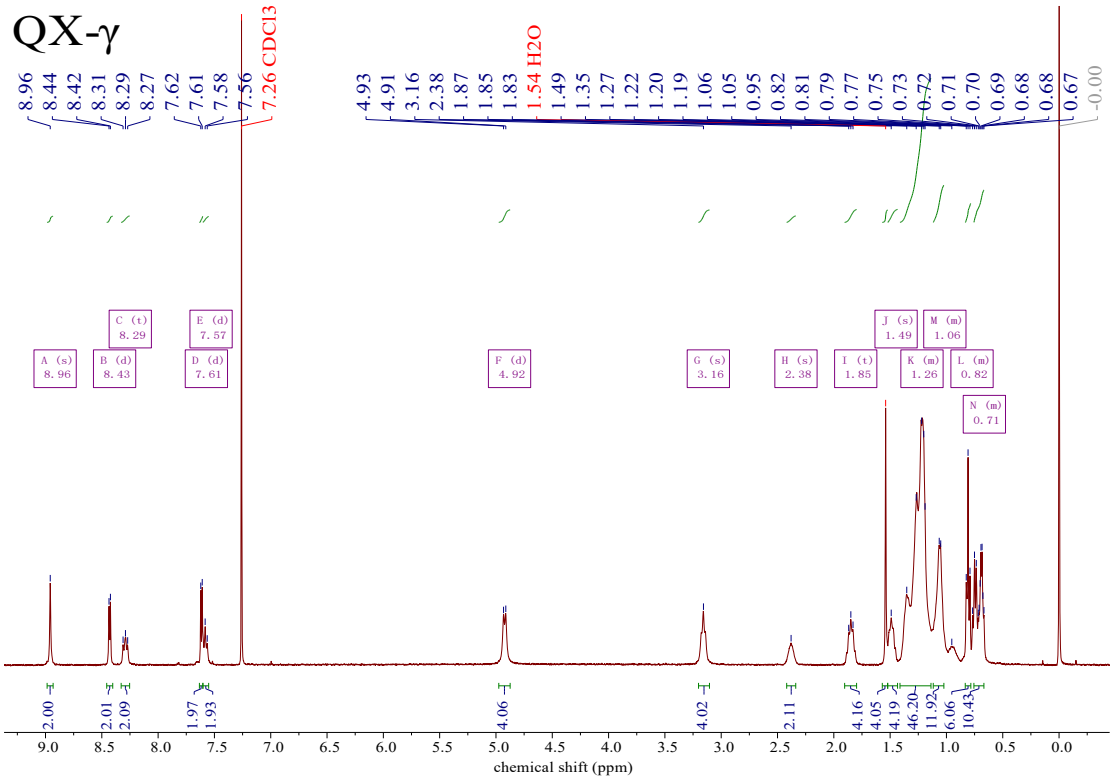

Figure S6. ^{1}H NMR spectrum of QX-γ in $CDCl_3$.

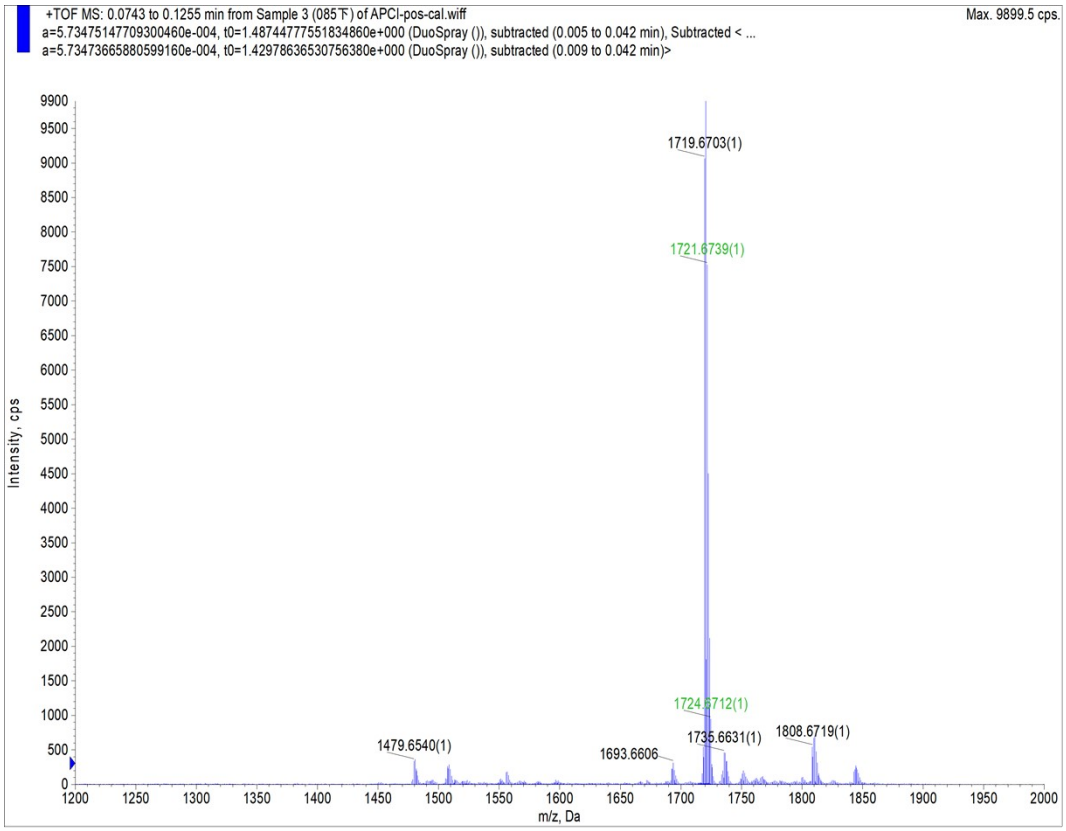

Figure S7. The high resolution time of flight mass spectrometer of QX-α.

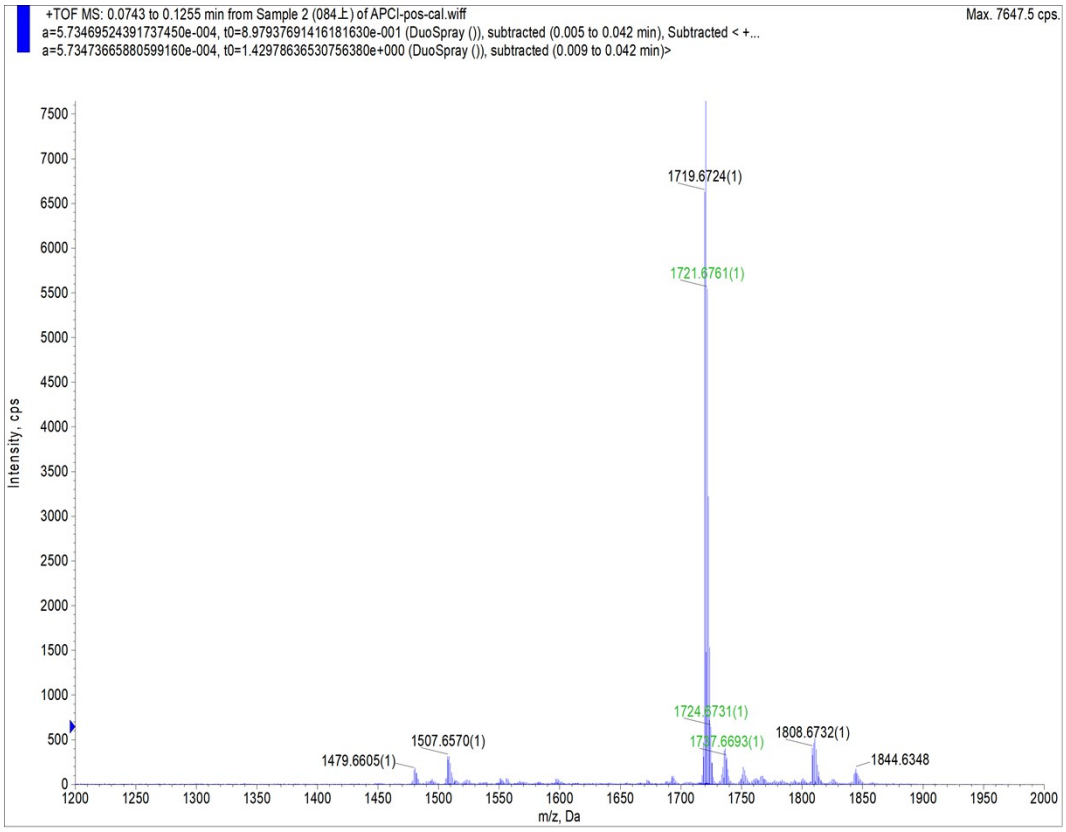

Figure S8. The high resolution time of flight mass spectrometer of QX-γ.

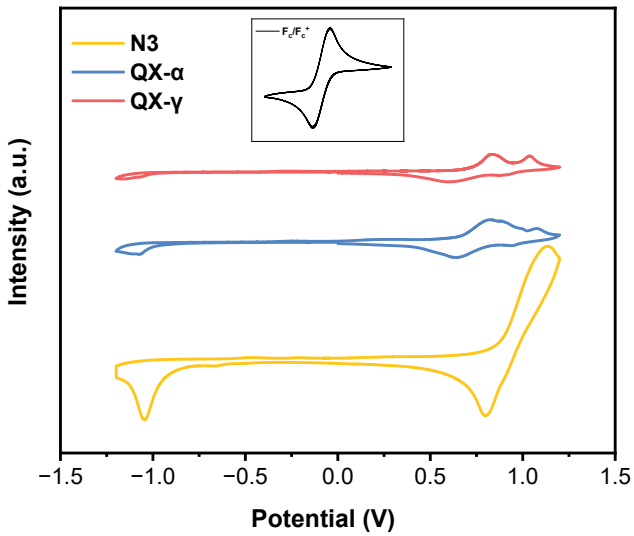

Figure S9. The CV curves of QX-α, QX-γ and N3.

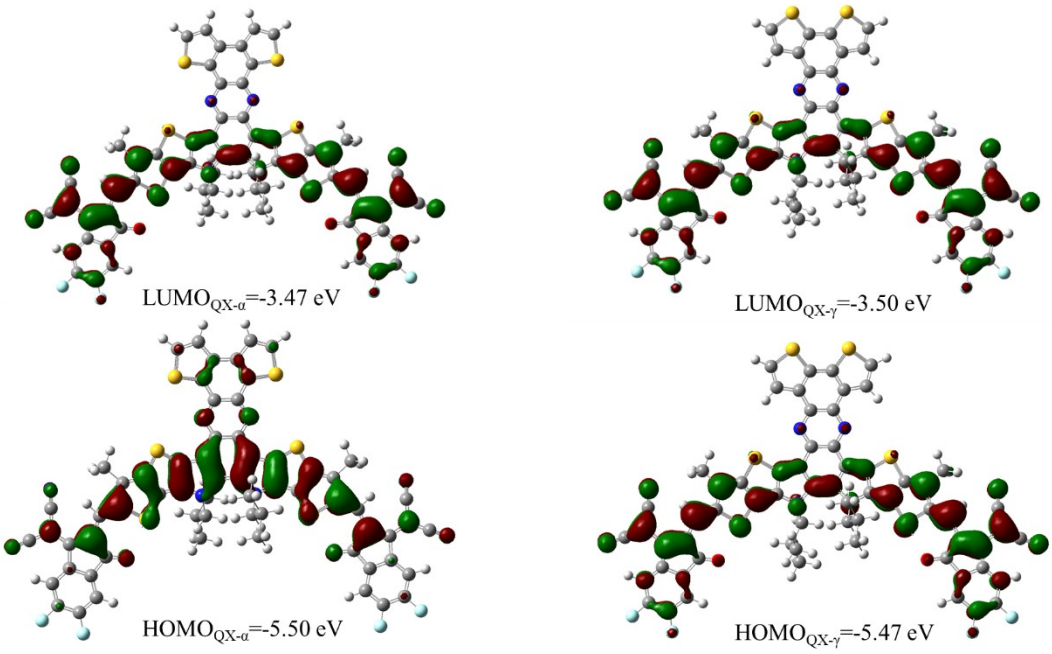

Figure S10. The distribution of HOMO and LUMO of QX-α and QX-γ.

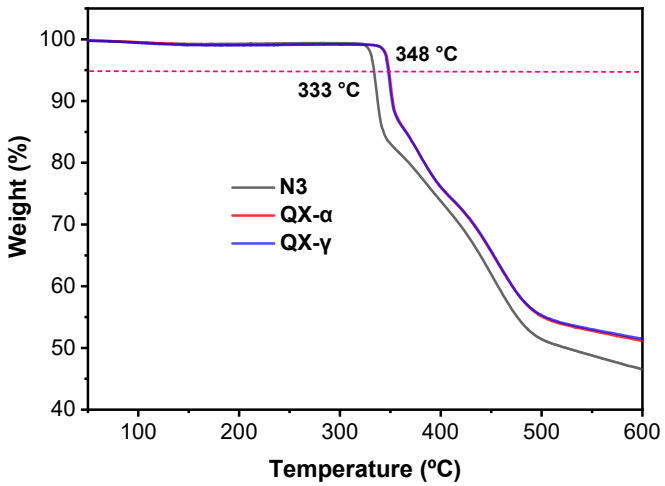

Figure S11. Thermogravimetric analysis (TGA) curves of N3, QX-α and QX-γ.

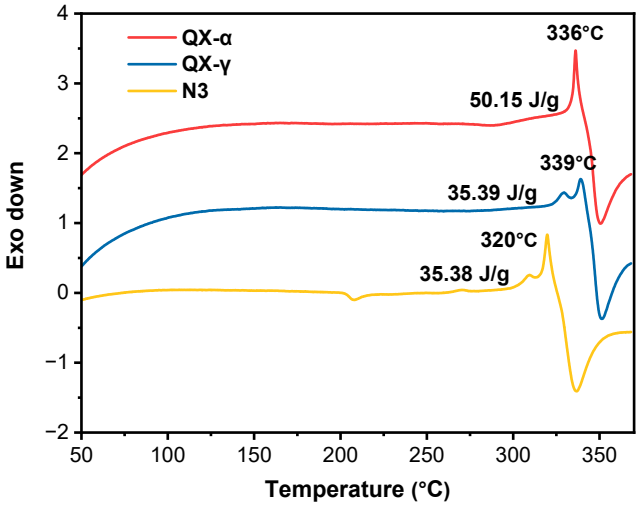

Figure S12. The first DSC heating-scan profiles from 30 to 380°C of pristine materials.

Table S1. Summarized contact angels and surface energies of D18, N3, QX-α and QX-γ.

Film	θ_{Water} [°]	Θ_{DIM} [°]	γ^d [mN m^{-1}]	γ^p [mN m^{-1}]	γ [mN m^{-1}]	γ_{D18-A} [mN m^{-1}]	$\gamma_{N3/A}$ [mN m^{-1}]	ω_{A2}
D18	95.07	58.98	27.045	1.544	28.60	/	/	/
N3	92.58	47.53	34.673	1.037	35.71	1.044	/	/
QX-α	90.36	45.41	35.429	1.378	36.81	1.135	0.055	-1.03
QX-γ	89.32	48.08	33.457	1.893	35.35	0.711	0.271	-0.42

Figure S13. Thin-layer chromatography (TLC) analysis of QX-α and QX-γ.

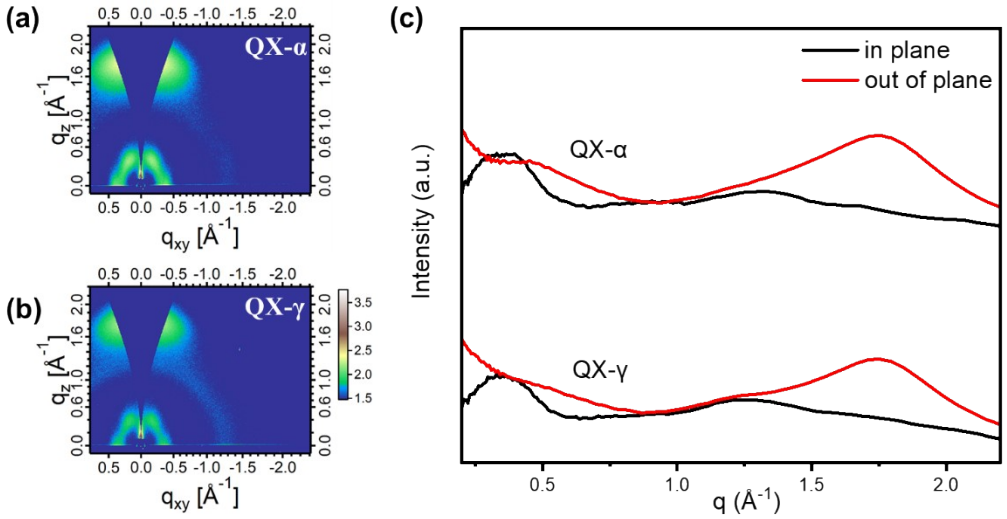

Figure S14. 2D GI-WAXS patterns of the neat films based on QX-α (a) and QX-γ (b), the corresponding curves (c).

Table S2. Detailed GI-WAXS peak information of the neat films.

Neat films	π-π stacking (OOP)				Lamellar stacking (IP)			
	q_Z (Å^{-1})	d (Å)	FWHM (Å^{-1})	CCL (Å)	q_{XY} (Å^{-1})	d (Å)	FWHM (Å^{-1})	CCL (Å)
QX-α	1.74	3.62	0.260	24.17	0.35	17.98	0.187	33.60
QX-γ	1.74	3.62	0.275	22.85	0.35	17.98	0.192	32.72

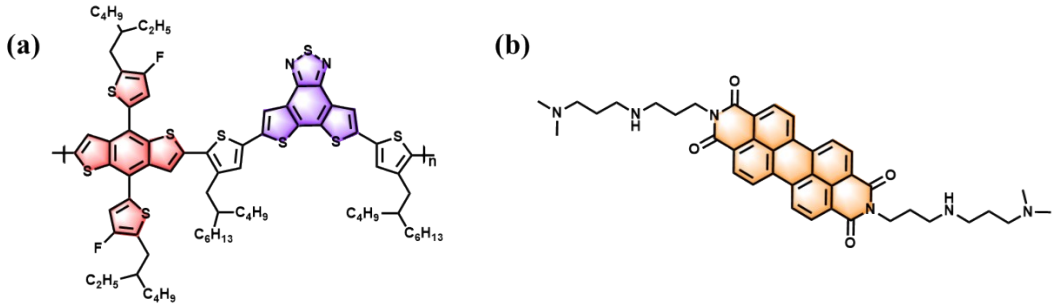

Figure S15. The chemical structure of molecules D18 (a) and PDINN (b).

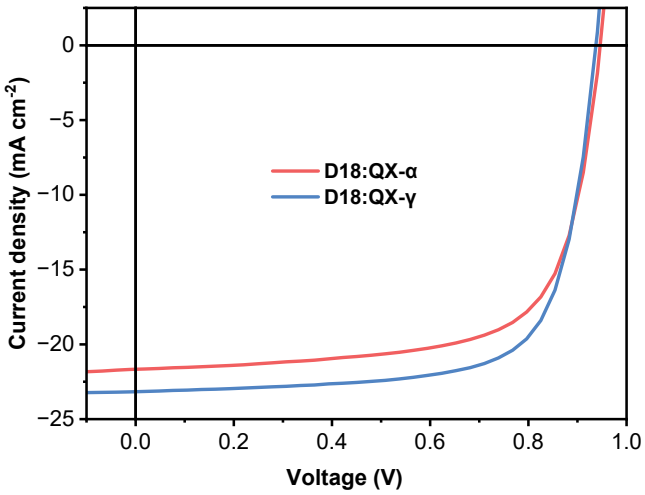

Figure S16. The *J*−*V* curves of the OSCs fabricated by D18:QX-α and D18:QX-γ.

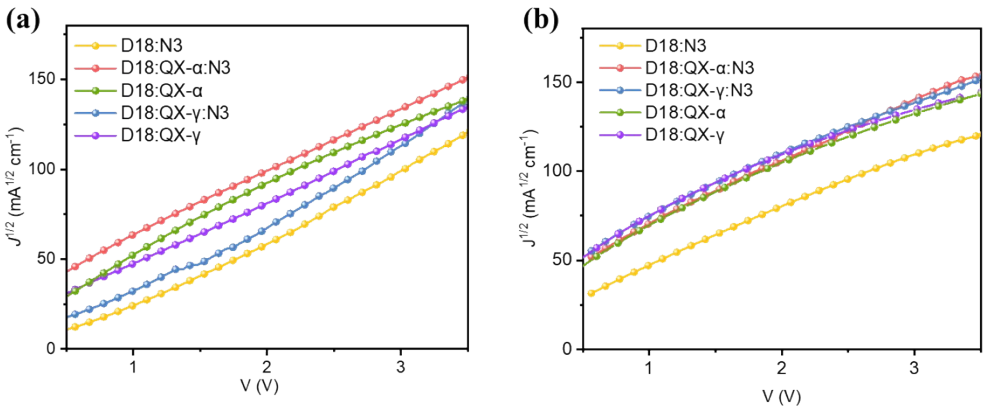

Figure S17. The electron mobilities (a) and the hole mobilities (b) of the devices.

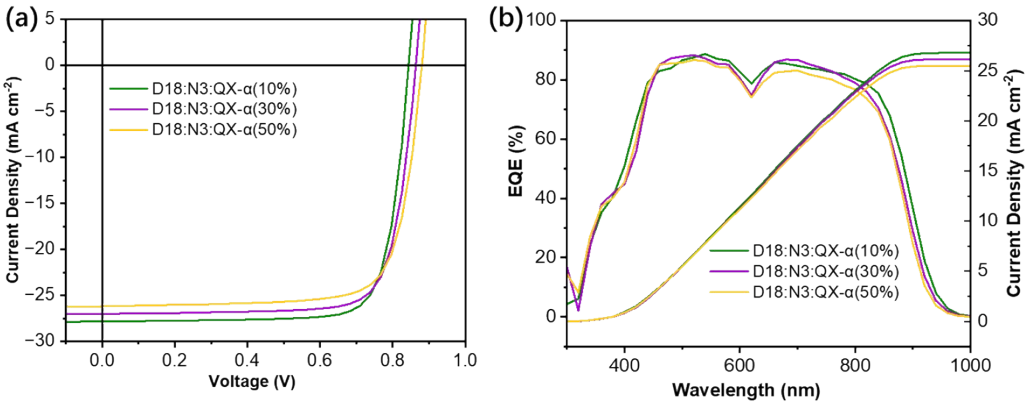

Figure S18. The *J*−*V* curves (a) and EQE curves (b) of devices fabricated by different ratios of QX-α in D18:N3.

Table S3. Photovoltaic parameters of the OSCs fabricated by different ratios of QX-α in D18:N3 under AM 1.5 G illumination at 100 mW cm^{-2}.

Active Layer	V_{OC} [V]	J_{SC}/J_{SC}^{cal} [mA cm^{-2}]	FF [%]	PCE^{max}
D18:N3:10%QX-α	0.845	27.80/26.73	79.23	18.63
D18:N3:20%QX-α	0.862	27.86/26.80	80.5	19.33
D18:N3:30%QX-α	0.864	27.00/26.17	78.12	18.21
D18:N3:50%QX-α	0.878	26.16/25.50	76.71	17.63

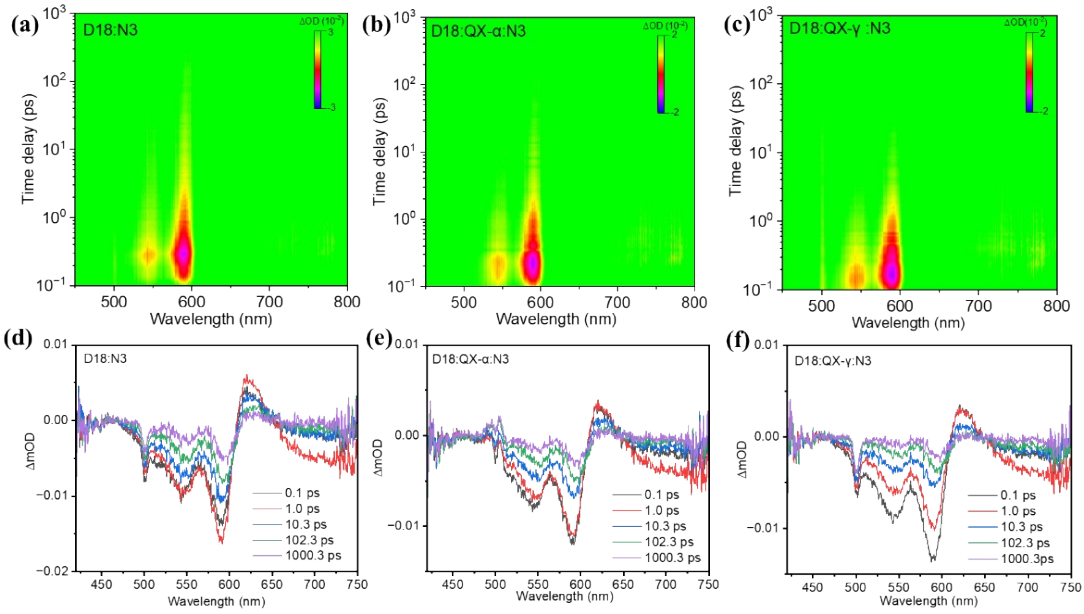

Figure S19. Color plot of transient absorption of blend film of D18:N3 (a), D18:N3:QX-α (b), and D18:N3:QX-γ (c). Representative spectra of blend films of D18:N3 (d), D18:N3:QX-α (e), and D18:N3:QX-γ (f) at indicated delay

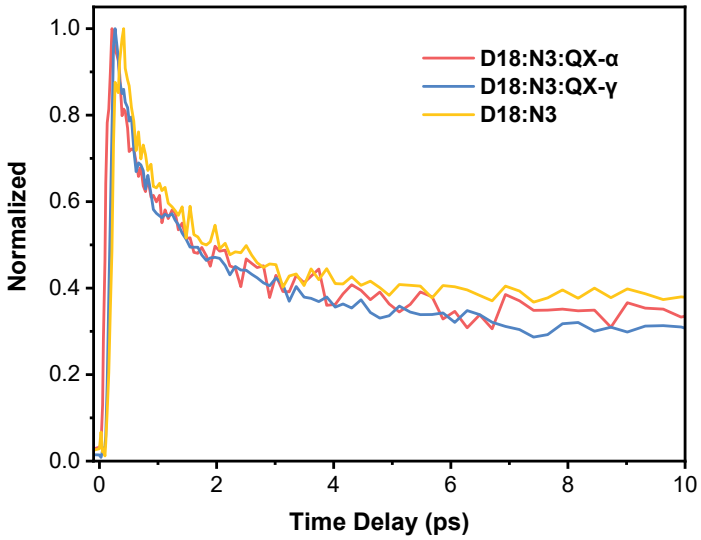

Figure S20. Decay dynamics monitored at the wavelength of 580 nm of blend films of D18:N3, D18:N3:QX-α, and D18:N3:QX-γ.

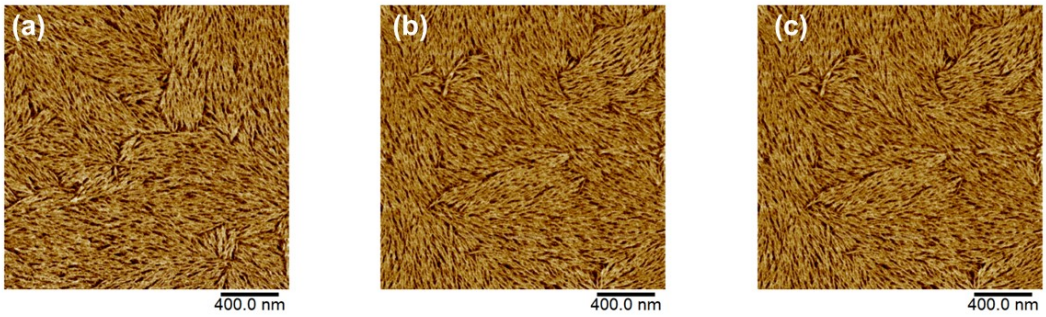

Figure S21. Phase images obtained by tapping-mode AFM for the blend films based on D18:N3 (a), D18:N3:QX-α (b), and D18:N3:QX-γ (c).

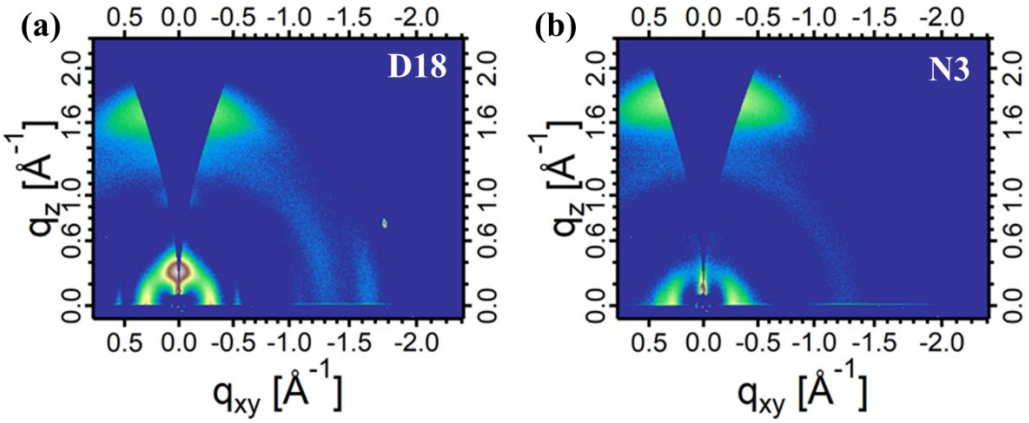

Figure S22. 2D GI-WAXS patterns of the neat films based on D18 (a) and N3 (b).

Table S4. Detailed GI-WAXS peak information of the blend films.

Blend films	π-π stacking (OOP)				Lamellar stacking (IP)			
	q_Z (Å^{-1})	d (Å)	FWHM (Å^{-1})	CCL (Å)	q_{XY} (Å^{-1})	d (Å)	FWHM (Å^{-1})	CCL (Å)
D18:N3	1.73	3.63	0.217	28.95	0.29	21.7	0.081	77.57
D18:N3:QX-α	1.73	3.63	0.221	28.43	0.29	21.7	0.085	73.92
D18:N3:QX-γ	1.73	3.63	0.220	28.56	0.29	21.7	0.076	82.68

Table S5. Detailed E_{Loss} parameters of the OSCs based on D18:N3 and D18:N3:20% QX-α.

BHJ	V_{oc} (V)	E_g (eV)	E_{loss} (eV)	ΔE_1 (eV)	ΔE_2 (eV)	ΔE_3 (eV)	EQE_{EL}

D18:N3	0.827	1.414	0.587	0.259	0.089	0.239	1.0×10^{-4}
D18:N3:QX-α	0.856	1.409	0.553	0.260	0.072	0.221	2.0×10^{-4}

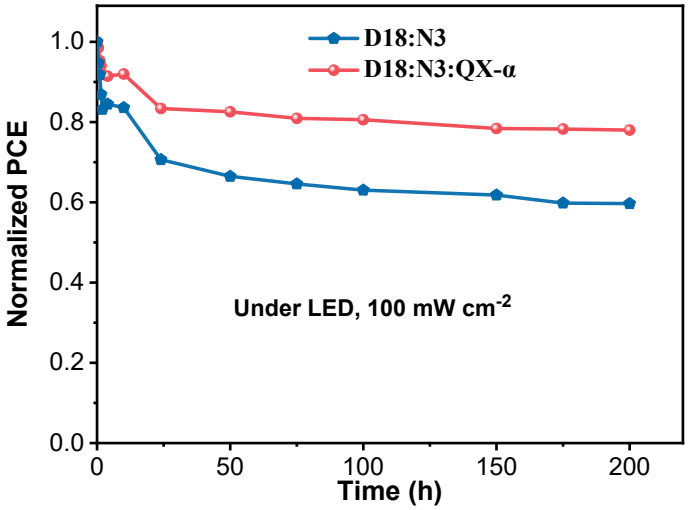

Figure S23. Normalized PCEs of the rigid OSCs device based on D18:N3 and D18:N3:QX-α storage under LED, 100 mW cm^{-2}.

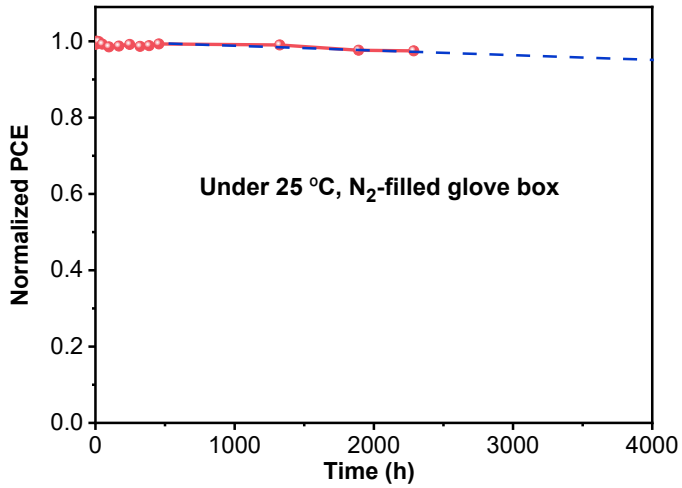

Figure S24. Normalized PCEs of the rigid OSCs device based on D18:N3:QX-α storage at 25 ºC in N_2–filled glove box over 2,287 hours. The dashed line corresponds to the linear fitting result from 200 hours to 2,000 h, partly excluding the influence of burn-in loss.

Table S6. Comparisons of PCE values of rigid ternary devices in the recent years.

Active layer	V_{OC} (V)	J_{SC} (mA cm^{-2})	FF (%)	PCE (%)	Ref.
D18:Y6:IDTT-SiO-IC	0.896	26.7	78.4	18.8	1
PM6:L8BO:BTP-S9	0.872	27.0	80.0	18.8	2
PM6:C9:isoIDTIC	0.866	27.3	80.4	19.0	3
PM6:L8BO:Y-C10ch	0.886	27.2	79.2	19.1	4
PM6:PTQ10:eC9	0.855	27.9	80.2	19.1	5
PM6:BTP-eC9:LA23	0.858	28.0	79.5	19.1	6
PM6:DAA-4	0.880	27.1	79.9	19.1	**7**
PM6:BTP-eC9:BTP-S16	0.863	27.7	80.6	19.3	8
D18:N3:QX-α	**0.862**	**27.9**	**80.5**	**19.3**	**This work**
D18:BTP-Cy-4F:BTP-eC9	0.925	26.1	80.3	19.4	9
PBQx-TCl:PM6:eC9-2Cl	0.886	27.2	81.1	19.5	10
PBTz-F:PM6:L8BO	0.905	27.2	79.3	19.5	11
PM6:D18:L8BO	0.896	26.7	81.9	19.6	12

Table S7. Comparisons of PCE values of flexible devices in the recent years.

Substrate	Bottom electrode	Active layer	PCE (%)	Ref.
PET	AgNWs/PH1000	D18-Cl:G19:Y6	15.9	13
PEN	ITO	PM6:BTP-eC9	16.0	14
PET	Ag NWs/PH1000	PM6:BTP-eC9:ZY-4Cl	16.1	15
PET	PH1000	PM6:Y6	16.6	16
PEN	ITO	PM6:BTP-eC9	16.7	17
PET	Em-Ag/AgNWs-IL	PM6:BTP-eC9:$PC_{71}BM$	17.5	18
PET	**AgNWs**	**D18:N3:QX-α**	**18.0**	**This work**

References

1. F. Meng, Y. Qin, Y. Zheng, Z. Zhao, Y. Sun, Y. Yang, K. Gao and D. Zhao, *Angew. Chem. Int. Ed.*, 2023, **62**, e202217173.
2. C. He, Q. Shen, B. Wu, Y. Gao, S. Li, J. Min, W. Ma, L. Zuo and H. Chen, *Adv. Energy Mater.*, **13**, 2204154.

3. Y. Lin, H. Chen, S. Y. Jeong, J. Tian, D. R. Naphade, Y. Zhang, M. Alsufyani, W. Zhang, S. Griggs, H. Hu, S. Barlow, H. Y. Woo, S. R. Marder, T. D. Anthopoulos and I. McCulloch, *Energy Environ. Sci.*, 2023, **16**, 1062-1070.
4. C. Xiao, X. Wang, T. Zhong, R. Zhou, X. Zheng, Y. Liu, T. Hu, Y. Luo, F. Sun, B. Xiao, Z. Liu, C. Yang and R. Yang, *Adv. Sci.*, 2023, **10**, e2206580.
5. R. Ma, X. Jiang, J. Fu, T. Zhu, C. Yan, K. Wu, P. Müller-Buschbaum and G. Li, *Energy Environ. Sci.*, 2023, DOI: 10.1039/d3ee00294b.
6. C. Han, J. Wang, S. Zhang, L. Chen, F. Bi, J. Wang, C. Yang, P. Wang, Y. Li and X. Bao, *Adv. Mater.*, 2023, **35**, e2208986.
7. S. Li, C. He, T. Chen, J. Zheng, R. Sun, J. Fang, Y. Chen, Y. Pan, K. Yan, C.-Z. Li, M. Shi, L. Zuo, C.-Q. Ma, J. Min, Y. Liu and H. Chen, *Energy Environ. Sci.*, 2023, DOI: 10.1039/d3ee00630a.
8. T. Chen, S. Li, Y. Li, Z. Chen, H. Wu, Y. Lin, Y. Gao, M. Wang, G. Ding, J. Min, Z. Ma, H. Zhu, L. Zuo and H. Chen, *Adv Mater*, 2023, **35**, 2300400.
9. M. Deng, X. Xu, Y. Duan, L. Yu, R. Li and Q. Peng, *Adv Mater*, 2023, **35**, 2210760.
10. P. Bi, J. Wang, Y. Cui, J. Zhang, T. Zhang, Z. Chen, J. Qiao, J. Dai, S. Zhang, X. Hao, Z. Wei and J. Hou, *Adv Mater*, 2023, **35**, 2210865.
11. B. Pang, C. Liao, X. Xu, L. Yu, R. Li and Q. Peng, *Adv Mater*, 2023, **35**, 2300631.
12. L. Zhu, M. Zhang, J. Xu, C. Li, J. Yan, G. Zhou, W. Zhong, T. Hao, J. Song, X. Xue, Z. Zhou, R. Zeng, H. Zhu, C.-C. Chen, R. C. I. MacKenzie, Y. Zou, J. Nelson, Y. Zhang, Y. Sun and F. Liu, *Nat. Mater.*, 2022, 21, 656-663.
13. Z. Chen, W. Song, K. Yu, J. Ge, J. Zhang, L. Xie, R. Peng and Z. Ge, *Joule*, 2021, **5**, 2395-2407.
14. X. Song, G. Liu, P. Sun, Y. Liu and W. Zhu, *J. Phys. Chem. Lett.*, 2021, **12**, 10616-10621.
15. Y. Sun, X. Duan, W. Song, J.-W. Qiao, X. Li, Y. Cai, H. Wu, J. Zhang, X.-T. Hao, Z. Tang, Z. Ge and F. Huang, *Energy Environ. Sci.*, 2022, **15**, 1563-1572.
16. J. Wan, Y. Xia, J. Fang, Z. Zhang, B. Xu, J. Wang, L. Ai, W. Song, K. N. Hui, X. Fan and Y. Li, *Nano-Micro. Lett.*, 2021, **13**, 44.
17. X. Liu, Z. Zheng, J. Wang, Y. Wang, B. Xu, S. Zhang and J. Hou, *Adv Mater*, 2022, **34**, 2106453.
18. G. Zeng, W. Chen, X. Chen, Y. Hu, Y. Chen, B. Zhang, H. Chen, W. Sun, Y. Shen, Y. Li, F. Yan and Y. Li, *J. Am. Chem. Soc.*, 2022, 144, 8658-8668.